NAC-Capped Quantum Dot as Nuclear Staining Agent for Living Cells via an In Vivo Steering Strategy

ARTICLE *in* THE JOURNAL OF PHYSICAL CHEMISTRY C · MARCH 2010

Impact Factor: 4.77 · DOI: 10.1021/jp908418v

7 AUTHORS, INCLUDING:

Dan Zhao
South-Central University For Nationalities
21 PUBLICATIONS **374** CITATIONS
SEE PROFILE

Zhike He
Wuhan University
144 PUBLICATIONS **2,450** CITATIONS
SEE PROFILE

Ricky Ngok-Shun Wong
Hong Kong Baptist University
199 PUBLICATIONS **3,750** CITATIONS
SEE PROFILE

Wing-Hong Chan
Hong Kong Baptist University
244 PUBLICATIONS **3,495** CITATIONS
SEE PROFILE

NAC-Capped Quantum Dot as Nuclear Staining Agent for Living Cells via an *In Vivo* Steering Strategy

Dan Zhao,[†] Zhike He,[†] Pui Shan Chan,[‡] Ricky N. S. Wong,[‡] Nai Ki Mak,*[,‡] Albert W. M. Lee,[§] and Wing Hong Chan*[,§]

Key Laboratory of Analytical Chemistry for Biology and Medicine (Ministry of Education), College of Chemistry and Molecular Sciences, Wuhan University, Wuhan 430072, and Departments of Biology and Chemistry, Hong Kong Baptist University, Kowloon Tong, Hong Kong SAR, China

Received: September 1, 2009; Revised Manuscript Received: February 5, 2010

We describe a new nuclear staining strategy by *in vivo* anchoring Hoechst 33342, a commonly used nuclear staining organic dye, onto water-soluble *N*-acetylcysteine (NAC)-capped CdTe quantum dots (QDs). The strong H-bonding and electrostatic interaction between the organic dye and the QDs entice the positively charged nuclear staining agent in carrying effectively the bright QDs into the nucleus of living cells. Dynamic confocal imaging studies indicated that all visible light emitting NAC-capped QDs with emitting wavelength ranging from 530 to 602 nm can be successfully targeted to the nucleus of the living cells within 30 min. The minimum quantity of Hoechst 33342 as the anchoring agent required in carrying QDs to the nucleus is found to be 5 μg/mL. In essence, a simple, fast, and specific bioimaging of the nucleus in living cells by QDs is accomplished.

1. Introduction

In the post genomic era, one of the most important challenges facing bioscience is the understanding of the complex spatial-temporal interplay of biomolecules in the cell environment. Cellular behavior has been a critical focus for the development of imaging technologies. Currently, many organelle specific fluorescent organic dyes were designed and developed; however, the photostability and the intensity of these dyes are far from satisfactory.[1–4] Organic fluorophores are also susceptible to photobleaching and their working lifetime for cell imaging purposes is detrimentally restrictive. Therefore, better and more stable fluorescent markers for cell imaging are in great demand.

Semiconductor nanoparticles (quantum dots) are a new class of materials suitable for imaging of biological materials. Quantum dot properties appealing to bioscientists include high quantum yield, high molar extinction coefficients, size-tunable optical and electronic properties, and broad absorption with narrow, symmetric photoluminescence (PL) spectra spanning the visible light to near-infrared. The potential uses of QDs for *in vivo* cellular imaging have been demonstrated and reviewed.[9–11] In great contrast to organic fluorescent dyes, these nanoparticles exhibit high resistance to photo- and chemical degradations.[5–7] In addition, reliable synthetic protocols of high-quality CdSe/CdS core/shell nanoparticles were also reported.[8] The preparation of hydrophobic QDs required fairly complicated laboratory manipulative skills and the use of toxic materials. Recently, direct synthesis of water-soluble thiol-capped CdTe QDs was achieved by both refluxing and hydrothermal processes.[12,13] By adopting the one-pot hydrothermal process and using *N*-acetylcysteine as the stabilizing agent, we have successfully synthesized high-quality water-soluble visible light emitting CdTe QDs and NIR emitting CdTe/CdS core/shell QDs. Furthermore, the cellular uptake of the as-prepared CdTe/CdS QDs by living cells was demonstrated by us.[14]

Hydrophilic QDs stabilized with thio-carboxylate capping agents have been rarely utilized alone as a specific nucleus-targeted imaging agent, except for very small QDs.[15] The general solution for this challenge is to modify the surface ligands or bioconjugate with targeted directing agents.[16–18] For instance, F. Chen et al. demonstrated the construction of a CdSe/ZnS QD−peptide conjugate that carries the SV40 large T antigen nuclear localization signal can accumulate in the cell nucleus.[17] However, this approach requires a fairly complicated experimental design and manipulation. Very recently, Xu et al. reported the method for nucleus internalization of 3-mercaptopropionic acid (MPA)-capped QDs. The process was induced by using 4′,6-diamino-2-phenylindole (DAPI) and UV-irradiation of the cells.[19] In the process of investigating the spatial-temporal uptake behavior of QDs in the living cell, we discovered that the organic nuclear staining dye Hoechst 33342 could rapidly steer the QDs penetrating into the nucleus of a living cell. Here, we report the development of a strategy for anchoring Hoechst 33342 onto the water-soluble NAC-capped CdTe QDs so as to confer them with the ability for nuclear labeling.

2. Experimental Section

2.1. Materials. Tellurium (reagent powder, 99.8%), thioglycolic acid (TGA), and *N*-acetylcysteine (NAC) were purchased from Sigma. $CdCl_2 \cdot H_2O$ and sodium borohydride ($NaBH_4$) were from Aldrich. Hoechst 33342 was obtained from Fluka. All chemicals were of the highest commercially available purity and used as received without further purification. Deionized distilled (DI) water prepared from a Milli-Q-RO4 water purification system (Millipore) was purged with nitrogen (N_2) for 30 min before use. All reagents were of analytical grade or above unless otherwise stated. The hydrothermal synthesis of visible

* Corresponding authors. Phone: +852-3411-7076 (W.H.C.); +852-3411-7059 (N.K.M.). Fax: +852-3411-7348 (W.H.C.); +852-3411-5995 (N.K.M.). E-mail: whchan@hkbu.edu.hk (W.H.C); nkmak@hkbu.edu.hk (N.K.M.).

[†] Wuhan University.

[‡] Department of Biology, Hong Kong Baptist University.

[§] Department of Chemistry, Hong Kong Baptist University.

10.1021/jp908418v
Published on Web 03/19/2010

SCHEME 1: Proposed Binding Model between NAC-CdTe QDs with Hoechst 33342 via Four H-Bonding

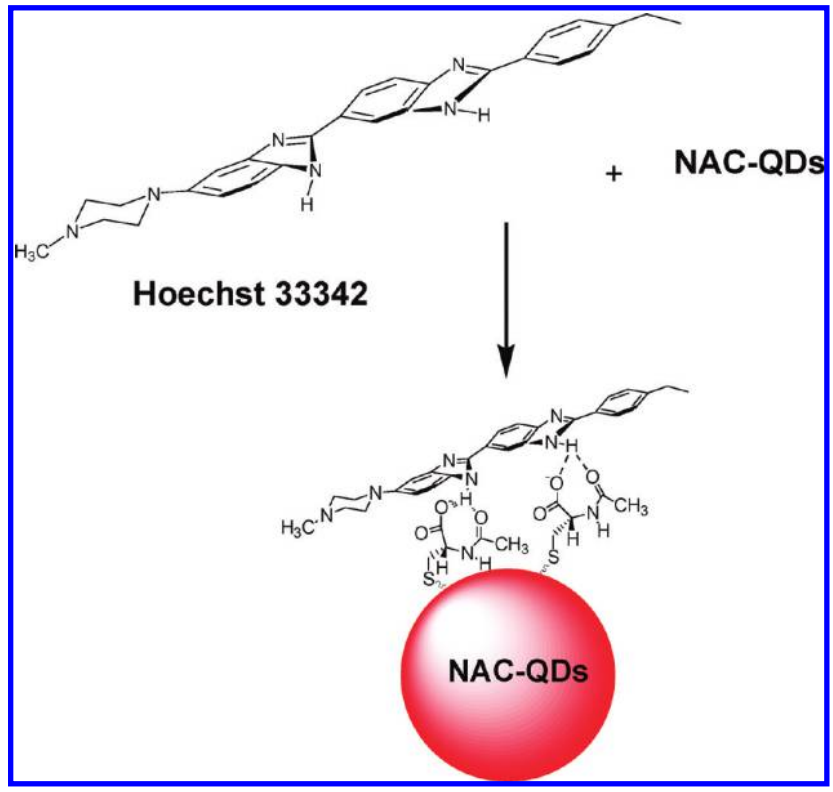

light and NIR emitting NAC-capped CdTe/CdS QDs was adopted from our in-house protocol.[14] By controlling the reaction time (i.e., from 40 to 65 min), different sizes of water-soluble QDs were prepared. To remove the excess NAC−Cd complexes at the end of the synthesis, cold 2-propanol was added to the reaction mixture to precipitate NAC-capped CdTe/CdS QDs. The as-prepared product was dried overnight under a vacuum at 40 °C and ready for further experiments.

2.2. *In Vitro* Fluorescent Titration. A 1 mg portion of NAC-capped CdTe QDs of different sizes was dissolved in 10 mL of DI. To 1 mL of the QD solution was added successively a 10 μL portion of Hoechst standard solution (1 g/L) until 100 μL was introduced. Upon addition of each portion of the dye solution, the fluorescence of the mixture was measured by a fluorescence spectrophotometer.

2.3. Confocal Microscopic Imaging of NAC-Capped CdTe QDs. HK-1 cells (1×10^5 cells) were seeded onto a coverslip in a 35 mm culture dish for overnight. The cells were incubated with QDs (100 μg/mL) in PBS for 1 h in the dark. The cells were then washed and stained with Hoechst 33342 (10 μg/mL) in PBS for 15 min in the dark. The emitted fluorescent signals of QDs and Hoechst 33342 were examined using an Olympus FV1000 confocal microscope equipped with a spectral detection system. A diode laser line at the 405 nm line was used for excitation of the Hoechst 33342 and QDs (ν_{max} = 530, 590, and 602 nm). A 543 nm helium−neon laser was used for the excitation of the NIR QDs (ν_{max} = 735 nm). Emission signals at 425−525 nm (Hoechst 33342), 520−570 nm (QDs ν_{max} = 530 nm), 572−672 nm (QDs ν_{max} = 590 nm), 590−640 nm (QDs ν_{max} = 602 nm), and 730−780 nm (QDs ν_{max} = 735 nm) were collected. A 60× oil immersion objective and pinhole size of 110 μm were used for image capturing. Images were processed and analyzed using the FV10-ASW software (Olympus).

2.4. Cell Culture. All cell cultures were incubated at 37 °C in a humidified incubator with 5% CO_2. Human nasopharyngeal carcinoma cells (HK-1) and African green monkey kidney cells (COS-7) were maintained in complete RPMI 1640 medium, whereas immortalized human keratinocyte cells (HaCaT) were maintained in complete DMEM medium. Both media were supplemented with 10% FBS (Gibco) and antibiotics (penicillin 50 U/mL; streptomycin 50 μg/mL). Human umbilical vein endothelial cells (HUVEC) were maintained in M199 medium supplemented with 20% heat-inactivated FBS, antibiotics (penicillin 50 U/mL; streptomycin 50 μg/mL), and 1% endothelial cell growth supplement (Upstate).

2.5. Staining with Hoechst 33342. Hoechst 33342 (Fluka) was dissolved in Milli-Q to give a stock solution of 2 mg/mL, and it was stored at 4 °C in the dark. The working solution (10 μg/mL) was freshly prepared by diluting the stock solution with PBS. The cells were then stained with Hoechst 33342 for 15 min at room temperature in the dark and then rinsed with PBS before confocal microscopic analysis.

3. Results and Discussion

3.1. Binding Model of NAC-Capped CdTe QDs and Hoechst 33342. In contrast to other commonly used mercaptocarboxylates such as thioglycolic acid (TGA) and MPA, NAC is not only able to confer the as-prepared QDs with good water solubility but also able to append an amide functionality on the surface of the nanoparticles. The appended α-amidocarboxylic moiety at the surface of the nanoparticles provides H-bonding binding sites for polar organic molecules including the nuclear staining agent Hoechst 33342. We envisage that the imidazole moieties of the dye could form multiple H-bonds with the hydrophilic QDs, as schematically shown in Scheme 1.[20]

The proposed binding model between QDs and Hoechst 33342 was substantiated by fluorescence titrations. Successive addition of Hoechst 33342 into NAC-capped QDs solution resulted in a remarkable fluorescence quenching of the nanoparticles. About 74% fluorescence reduction of the QDs with λ_{em} = 592 nm was observed when 0.1 equiv (by weight) of the

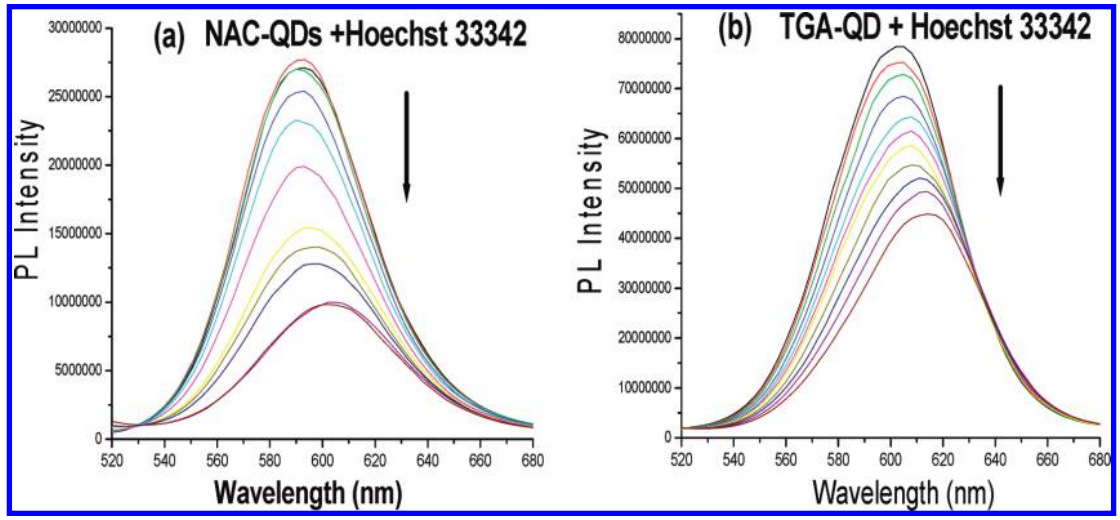

Figure 1. Fluorescence titrations between Hoechst 33342 and (a) NAC-CdTe QDs and (b) TGA-CdTe QDs in PBS buffer solution. From top to bottom, the concentrations of added Hoechst 33342 are 0, 1, 2, 3, 4, 5, 6, 7, 8, 9, and 10 μg/mL.

Hoechst 33342 was introduced (Figure 1a). In addition, a bathochromic shift of ~10 nm on the QD emissive peak was found, presumably triggered by the formation of a complex between the QD and Hoechst 33342. The slight enlargement of the complex in comparison with the native QDs corroborates nicely with the observed red-shift. Detailed studies revealed that the binding affinity of Hoechst 33342 to NAC-capped QDs is independent of the size of the nanoparticles. Irrespective of the size of the QDs used ranging from 2.6 to 5.5 nm (i.e., visible light or NIR emitting QDs), the described photophysical changes of the nanoparticles occurred invariantly when the QDs were mixed with Hoechst 33342. The rigid and fully conjugated π-system of the dyes enables them to serve as an effective electron acceptor or as an electron donor. The association of QDs and Hoechst 33342 via H-bonding upon irradiation can facilitate the photoinduced electron transfer process (PET), resulting in considerable quench of the PL of the QDs.[21,22] On the other hand, when 0.1 equiv (by weight) of the dye was mixed with QDs, the emission peak of Hoechst 33342 was completely turned off (results not shown). Thus, the mutual interaction between the NAC-capped QDs and Hoechst 33342 has been verified.

To confirm the uniqueness of NAC as a unique capping agent in the study, the same experiment was performed with the use of TGA-capped CdTe QDs. Only ~50% reduction of the PL of the QDs was evident when they were mixed with 0.1 equiv (by weight) of the Hoechst 33342 (Figure 1b). Without the presence of the α-amido group in the capping agent, the appended carboxylate groups on the surface of TGA-capped QDs can bind only moderately with Hoechst 33342, resulting in a much reduced quenching effect on the host nanoparticles.

3.2. Bioimaging of NAC-Capped CdTe QDs in Living Cells. After demonstrating the binding characteristics between QDs and Hoechst 33342, we then investigated the nuclear targeting of NAC-capped CdTe QDs to the nucleus of a living cell. HK-1 cells were exposed to NAC-capped QDs of various sizes (i.e., with emission peaks at 530, 590, 602, and 735 nm, respectively) and the fluorescent images of QD labeled cells were observed at 60 min after incubation. Both visible and NIR light emitting NAC-capped CdTe QDs were found internalized by the cells (Figure 2). Apparently, the hydrophilic property of the QDs did not prevent the penetration of the nanoparticles through the cell membrane. It is noteworthy that even the NIR emitting QDs with a diameter of ~5.5 nm can be taken up by

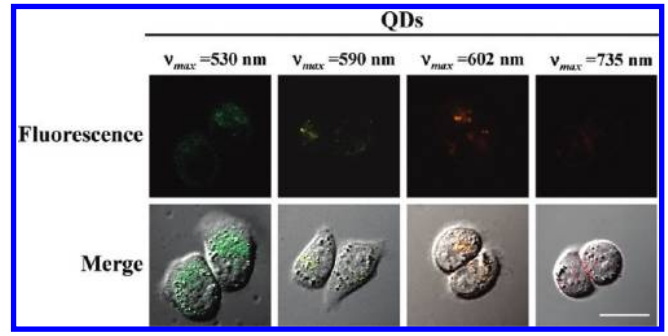

Figure 2. Confocal microscopic images of NAC-capped CdTe QDs in HK-1 cells. The cells were incubated with QDs in PBS (pH 7.4) for 1 h before capturing the confocal images. Upper panel: fluorescent images of QDs. Lower panel: the combined images of fluorescent signals from QDs and the bright field images of the cells. Scale bar: 20 μm.

the cells. The confocal images also showed that QDs of various sizes were localized mainly in the cytoplasm of the cells.

3.3. Nuclear Staining by Hoechst 33342 Steered NAC-Capped CdTe QDs. To define the scope and the limitations of the proposed technique in nuclear targeted bioimaging, four fundamental questions must be addressed: (1) what is the size limitation in QDs for the nucleus internalization; (2) what is the quenching effect between the nuclear staining agent Hoechst 33342 and the costained QDs; (3) what are the conditions required for cellular entry and nuclear delivery of QDs; and (4) what is the minimum quantity of Hoechst 33342 that can carry QDs to the nucleus? We envisage that Hoechst 33342 after coordinating with the QDs could still penetrate into the nucleus of the cells. To lay down the foundation for our study, as the negative controls, the confocal images of HK-1 cells labeled with only Hoechst 33342 were collected at different fluorescent signal ranges corresponding to the emission signal of Hoechst 33342 and the four different sizes of QDs used, respectively. Results from Figure 3a showed that the fluorescent signal of the control was very weak at 520−570 nm, and the signal was basically not detected at 570 nm and above. The results suggested that the contribution of emission signal from Hoechst 33342 to the quantum dot channel was negligible. To demonstrate the "steering effect" of Hoechst 33342 in directing the QDs to the nucleus of a living cell, cells labeled with various sizes of QDs were allowed to further incubate with Hoechst 33342 for 15 min. The emitted fluorescent signals of QDs and

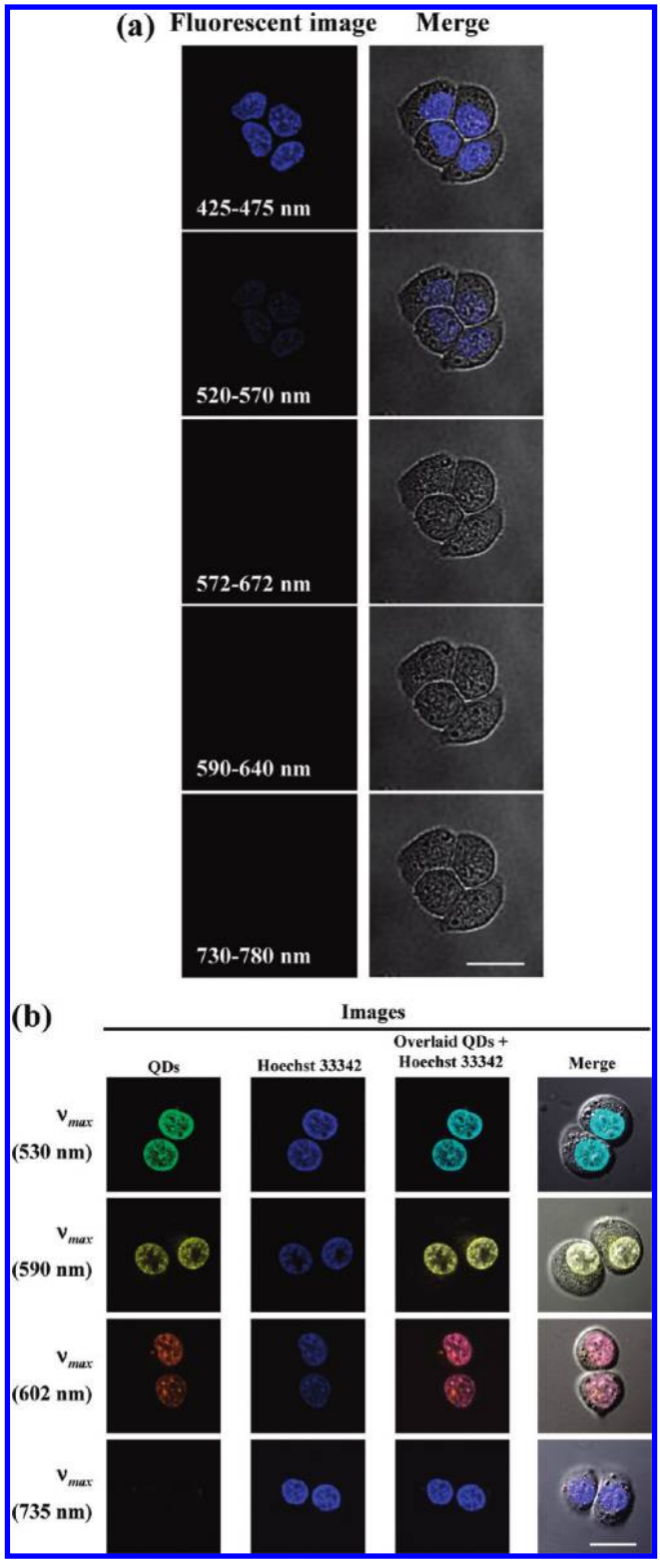

Figure 3. Confocal images of cells labeled with Hoechst 33342 in the presence or absence of NAC-QDs. (a) HK-1 cells were incubated with Hoechst 33342 for 15 min. Fluorescent signals at 425−475, 520−570, 572−672, 590−640, and 730−780 nm were then separately collected. The signal range was corresponding to the emission signal of Hoechst 33342, QDs (ν_{max} = 530 nm), QDs (ν_{max} = 590 nm), QDs (ν_{max} = 602 nm), and QDs (ν_{max} = 735 nm). (b) HK-1 cells were incubated with various sizes of QDs in PBS (pH 7.4) for 1 h followed by incubation with Hoechst 33342 for 15 min. The emitted fluorescent signals of QDs and Hoechst 33342 were examined using a confocal microscope as described in the Experimental Section. Scale bar: 20 μm.

Hoechst 33342 were separately collected, and the subcellular localization of QDs was determined by overlapping the fluorescent images of QDs with Hoechst 33342. A clear pattern of nuclear colocalization of QDs (ν_{max} = 530 nm) and Hoechst 33342, as judged from the overlapping of the fluorescent signals of QDs (green) and the nuclear dye Hoechst 33342 (blue), was seen (Figure 3b). Nuclear localization of QDs with a larger size (ν_{max} = 590 nm and ν_{max} = 602 nm) was also seen. However, a few QDs were also found in the cytoplasm of the cell. Unlike the visible light emitting QDs, the NIR light emitting QDs (ν_{max} = 735 nm) remained in the cytoplasm of the cells.

To further confirm whether the QDs were fully internalized into the nucleus, we performed vertical section scanning along the *Z*-axis. Under the influence of Hoechst 33342, nucleus localization of visible light emitting QDs was evident. A typical *z* section of HK-1 cells treated with NAC-QDs (ν_{max} = 530 nm) and the Hoechst dye is reported in Figure S1 of the Supporting Information. Using the same staining strategy, the enhancing effect of Hoechst 33342 on the nuclear localization of QDs could also be demonstrated by other different types of cell lines such as immortalized human keratinocyte (HaCaT cells), human umbilical vein endothelial cells (HUVEC), and African green monkey kidney cells (COS-7) (Figure S2, Supporting Information). Thus, the general applicability of this nuclear staining strategy has been established.

To address the question on the process of cellular uptake of QDs, HK-1 cells were pretreated with sodium azide, an agent known to inhibit cellular respiration, for 1 h before the treatment with QDs. Cytoplasmic uptake of QDs was greatly reduced in cells with sodium azide pretreatment (Figure S3a, Supporting Information). In addition, the cellular uptake of QDs also appears to be temperature dependent. The amount of cytoplasmic QDs was greatly reduced when the incubation was kept at 4 °C. These results indicated that the process of cellular uptake of QDs is temperature dependent and required the generation of metabolic energy. To further address the question on the metabolic energy/temperature requirement for the translocation of QDs from the cytoplasm to the nucleus, HK-1 cells were first incubated with QDs at 37 °C for 1 h to allow the normal entry of QDs into the cytoplasm. The cells were then treated with sodium azide for 1 h before the addition of Hoechst 33342. The results in Figure S3b of the Supporting Information clearly showed that Hoechst 33342-mediated nuclear localization of QDs was not affected by sodium azide. This observation suggested that the process of Hoechst 33342-mediated nuclear localization of QDs is independent of the process of cellular respiration. In contrast, the process of Hoechst 33342-mediated nuclear localization of QDs was inhibited at 4 °C. Taken together, these observations suggested that the cellular entry of QDs and the subsequent Hoechst 33342-mediated nuclear localization of QDs are a temperature dependent process.

To further determine the minimum quantity of Hoechst 33342 which can facilitate the nuclear localization of QDs, QD labeled cells were treated with various concentrations of the Hoechst dye. The results in Figure 4 showed the Hoechst-dye-dependent localization of QDs in the nucleus. At a lower concentration of Hoechst 33342 (2.5 μg/mL), QDs were mainly found in the cytoplasm of the cells. Increasing the concentration of Hoechst 33342 resulted in the increased nuclear localization of the QDs. The optimum dose of QDs for the nuclear localization was 10 μg/mL. To further support our observation that the emission signals obtained from QDs was not due to the leaking of the emission from Hoechst 33342, a lambda scan from 420 to 800 nm, with an interval of 20 nm, was performed on the Hoechst-

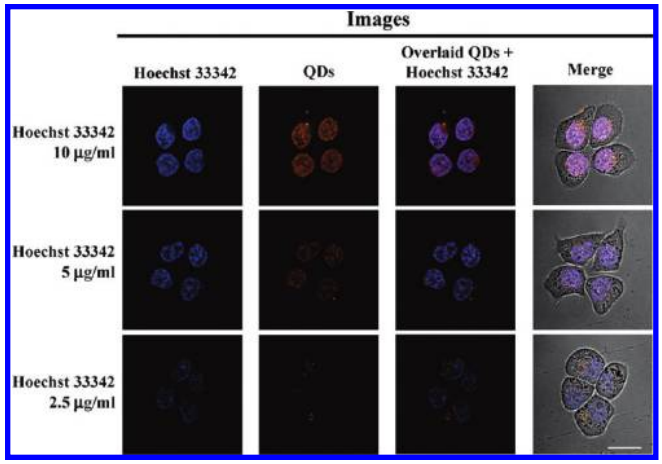

Figure 4. Effect of Hoechst 33342 on the nuclear location of the QDs (ν_{max} = 602 nm). QD (ν_{max} = 602 nm) labeled cells were treated with Hoechst 33342 (2.5−10 μg/mL) for 15 min. Scale bar: 20 μm.

TABLE 1: Fluorescent Emitted Maxima, Size, and Relative Volume of Different NAC-Capped CdTe QDs Employed in the Staining Experiments

type of QDs	emission maxima (nm)	size of the QDs[25] (diameter, nm)	volume ratio
NAC-QDs	530	2.57	V_0
NAC-QDs	590	3.24	$2.0V_0$
NAC-QDs	602	3.50	$2.5V_0$
NAC-QDs	735	5.48	$9.7V_0$

33342-stained HK-1 cells. The results from Figure S4 of the Supporting Information showed that the fluorescent signal was very weak at 480−540 nm, and the signal was basically not detected at 540 nm and above. The results suggested that the likelihood of Hoechst emission contributing to the QD channel can be completely ruled out.

We owed an explanation to rationalize the inability of the NIR-emitting QDs to accumulate into the nucleus of living cells under the influence of the dyes. Considering the fact that the diameter of the nuclear pore complex is 20−50 nm depending on the cell line,[23,24] NIR emitting QDs with a diameter of ~5.5 nm (i.e., core size) are small enough to penetrate through the nuclear membrane. As the size of the NIR-emitting QDs is substantially larger than those of the visible light emitting QDs, a longer incubation time was then given for Hoechst 33342 to interact and steer the relatively heavier QDs into the nucleus. Extending the incubation time of QD (ν_{max} = 735 nm) labeled cells with Hoechst 33342 from 15 to 60 min, however, had no significant effect in increasing the nuclear localization of the QDs in the cells (data not shown). Comparing the relative size of the NIR-emitting QDs (ν_{max} = 735 nm) with the size of a nuclear pore, QDs should in principle comfortably internalize into the nucleus. The inability of NIR-emitting QDs entering the nucleus of the cell could conceivably be due to the weight factor of the QDs. Simple calculation shows that the total volume and thus the mass of the NIR-emitting QD (ν_{max} = 735 nm) is 9.7-fold that of the visible light emitting QDs (ν_{max} = 530 nm) (Table 1). The electrostatic attractions between the DNA molecules and Hoechst 33342 perhaps are probably not strong enough to attract the heavier NIR-emitting QDs (ν_{max} = 735 nm) to the nucleus of the cell.

3.4. Dynamic Features of the Nuclear Labeling Process. In order to have a clear picture on the dynamic feature of this nuclear labeling process upon addition of the Hoechst dye, the image on the accumulation of NAC-QDs in the nucleus was captured continuously. The time-lapse images of QD accumulation in HK-1 cells are shown in Figure 5, and the video clip on the whole staining process is shown in the Supporting Information. As the nanosize QDs are dispersed in the cytoplasm, the overall fluorescent signal detected in the cytoplasm is very low (Figure 5a). In the presence of Hoechst 33342, NAC-QDs are rapidly accumulated in the nucleus (Figure 5b−e). The fast dynamic nature on the accumulation of QDs in the nucleus is quite apparent. After a duration of 20 min, the nucleus was brightly stained with QDs. It is worth noting that a small amount of QDs was detected in the nucleus at T = 0 min (Figure 5a). This is due to about a 5 min delay between the addition of Hoechst 33342 and the adjustment of instrument setting/refocusing of the cell for image capturing.

As shown in Scheme 1 and Figure 1, Hoechst 33342 forms complexes with NAC-QDs and this will result in fluorescence quenching of the nanoparticles. However, after steering of the QDs into the nucleus, a bright fluorescent image of the nucleus was observed. As Hoechst 33342 is a strong DNA binding agent,

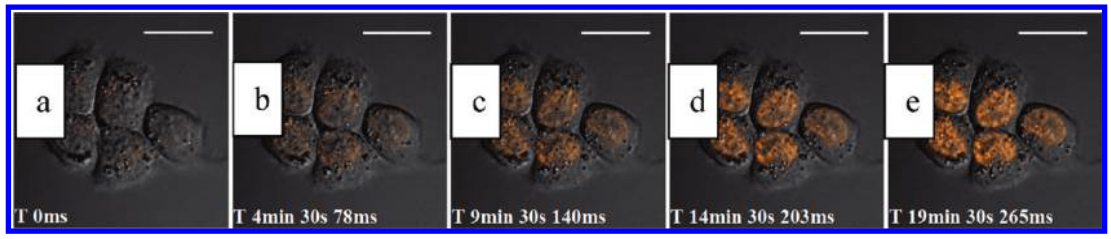

Figure 5. Time-lapse images of QDs (ν_{max} = 602 nm) in HK-1 cells. QD (ν_{max} = 602 nm) labeled cells were treated with Hoechst 33342 (10 μg/mL). Time-lapse recording of the fluorescence signal was performed with the image acquisition at every 30 s. Scale bar: 20 μm.

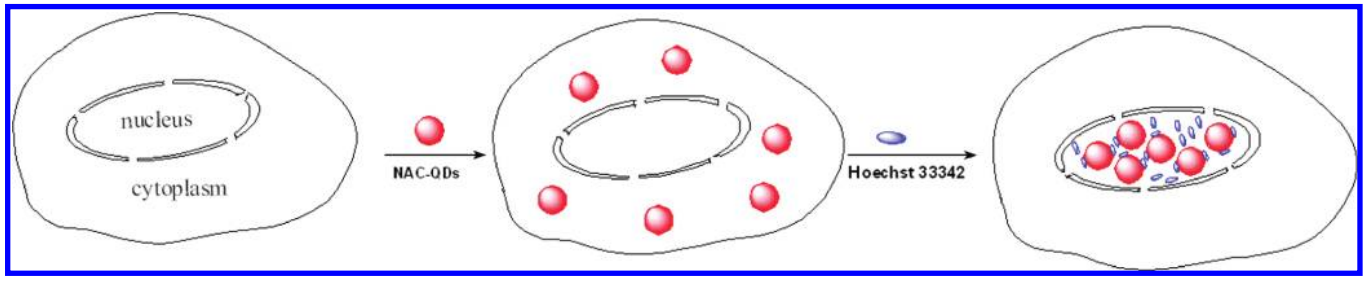

Figure 6. Using Hoechst anchored NAC-capped QDs as nuclear labeling agents for living cells.

the reassociation of Hoechst 33342 with the nuclear DNA might reduce the quenching effect of the Hoechst dye on the QDs. This hypothesis was further verified from the *in vitro* study using a cell-free system. Hoechst 33342 and NAC-QD complexes were exposed to an increasing concentration of DNA, and the PL of QDs was measured. The results in Figure S5 of the Supporting Information clearly showed a DNA-dose-dependent increase in PL, indicating the dissociation of the Hoechst dye from the QD complex.

4. Conclusion

In conclusion, we have developed a novel labeling technique to specifically target visible light emitting NAC-capped CdTe QDs into the nucleus of living cells. The crucial step involved in this new bioimaging strategy is to allow intracellular conjugation of an appropriate size of visible QDs (e.g., $\nu_{max} =$ 530−602 nm) with Hoechst 33342, resulting in steering the cytoplasmic QDs into the nucleus of living cells (Figure 6). It is worth noting that TGA- or MPA-capped CdTe QDs however were proved to be unable to accomplish this nuclear labeling purpose. In contrast to the previously reported nucleus labeling protocol,[15] our approach is mechanistically clear and the requirement of irradiating the cells with damaging UV light is not required. Our investigation revealed that QDs of different emission colors can be translocated from cytoplasm to the nucleus of the cell by a commonly used Hoechst 33342. In addition to the bioimaging, this technique has potential for other biomedical and biological applications, such as the guiding of nanoparticle enclosed chemotherapeutic drugs to the nucleus.

Acknowledgment. This work was supported by the Research Committee of the Hong Kong Baptist University (FRG2/08-09/073), the National Science Foundation of China (90717111), and the Science Fund for Creative Research Groups of NSFC (20621502).

Supporting Information Available: *Z*-axis scanning images of HK-1 cells treated with NAC-QDs and Hoechst 33342, nuclear delivery of QDs in different cell lines, effect of sodium azide and low incubation temperature on cell uptake of QDs, lambda scan of Hoechst 33342 stained HK-1 cells, effect of addition of ct-DNA on the PL of NAC-QD−Hoechst conjugate, and a video clip on the staining process. This material is available free of charge via the Internet at http://pubs.acs.org.

References and Notes

(1) Agorastos, N.; Borsig, L.; Renard, A.; Antoni, P.; Viola, G.; Spingler, B.; Kurz, P.; Alberto, R. *Chem. Eur. J.* **2007**, *13*, 3842–3852.
(2) Kubota, Y. *Bull. Chem. Soc. Jpn.* **1990**, *63*, 758–764.
(3) Shapiro, A. B.; Fox, K.; Lee, P.; Yang, Y. D.; Ling, V. *Int. J. Cancer* **1998**, *76*, 857–864.
(4) Li, W.; Yang, X.; Wang, K.; Tan, W.; He, Y.; Guo, Q.; Tang, H.; Liu, J. *Anal. Chem.* **2008**, *80*, 5002–5008.
(5) Murphy, C. J. *Anal. Chem.* **2002**, *74*, 520A–526A.
(6) Niemeyer, C. M. *Angew. Chem., Int. Ed. Engl.* **2001**, *40*, 4128–4158.
(7) Alivisatos, P. *Nat. Biotechnol.* **2004**, *22*, 47–52.
(8) Li, J. J.; Wang, Y. A.; Guo, W.; Keay, J. C.; Mishima, T. D.; Johnson, M. B.; Peng, X. *J. Am. Chem. Soc.* **2003**, *125*, 12567–12575.
(9) Chen, F.; Gerion, D. *Nano Lett.* **2004**, *4*, 1827–1832.
(10) Smith, A. M.; Gao, X.; Nie, S. *Photochem. Photobiol.* **2004**, *80*, 377–385.
(11) Medintz, I. L.; Uyeda, H. T.; Goldman, E. R.; Mattoussi, H. *Nat. Mater.* **2005**, *4*, 435–446.
(12) Zou, L.; Gu, Z.; Zhang, N.; Zhang, Y.; Fang, Z.; Zhu, W.; Zhong, X. *J. Mater. Chem.* **2008**, *18*, 2807–2815.
(13) Zhang, H.; Wang, L.; Xiong, H.; Hu, L.; Yang, B.; Li, W. *Adv. Mater.* **2003**, *15*, 1712–1715.
(14) Zhao, D.; He, Z.; Chan, W. H.; Choi, M. M. F. *J. Phys. Chem. C* **2009**, *113*, 1293–1300.
(15) Nabiev, I.; Mitchell, S.; Davies, A.; Williams, Y.; Kelleher, D.; Moore, R.; Gun'kp, Y. K.; Byrne, S.; Rakovich, Y. P.; Donegan, J. F.; Sukhanova, A.; Conroy, J.; Cottell, D.; Gaponik, N.; Rogach, A.; Volkov, Y. *Nano Lett.* **2007**, *7*, 3452–3461.
(16) Hoshino, A.; Fujioka, K.; Oku, T.; Nakamura, S.; Suga, M.; Yamaguchi, Y.; Suzuki, K.; Yasuhara, M.; Yamamoto, K. *Microbiol. Immunol.* **2004**, *48*, 985–994.
(17) Chen, F.; Daniele, G. *Nano Lett.* **2004**, *4*, 1827–1832.
(18) Rozenzhak, S. M.; Kadakia, M. P.; Caserta, T. M.; Westbrook, T. R.; Stone, M. O.; Naik, R. R. *Chem. Commun.* **2005**, 2217–2219.
(19) Xu, Y.; Wang, Q.; He, P.; Dong, Q.; Liu, F.; Liu, Y.; Lin, L.; Yan, H.; Zhao, X. *Adv. Mater.* **2008**, *20*, 3468–3473.
(20) Parkinson, J. A.; Ebrahimi, S. E.; Mckie, J. H.; Douglas, K. T. *Biochemistry* **1994**, *33*, 8442–8452.
(21) Zhao, D.; Chan, W. H.; He, Z.; Qiu, T. *Anal. Chem.* **2009**, *81*, 3537–3543.
(22) Shen, J.-S.; Yu, T.; Xie, J.-W.; Jiang, Y.-B. *Phys. Chem. Chem. Phys.* **2009**, *11*, 5062–5069.
(23) Fahrenkrog, B.; Aebi, U. *Nat. Rev. Mol. Cell Biol.* **2003**, *4*, 757–766.
(24) Liu, Y.; Shipton, M. K.; Ryan, J.; Kaufman, E. D.; Franzen, S.; Feldheim, D. L. *Anal. Chem.* **2007**, *79*, 2221–2229.
(25) Yu, W. W.; Qu, L.; Guo, W.; Peng, X. *Chem. Mater.* **2003**, *15*, 2854–2860.

JP908418V